PERGAMON

Vision Research 39 (1999) 1611–1630

Vision Research

Seeing better at night: life style, eye design and the optimum strategy of spatial and temporal summation

Eric J. Warrant *

Institute for Advanced Study, Wallotstrasse 19, D-14193 Berlin, Germany

Received 16 February 1998; received in revised form 10 June 1998

Abstract

Animals which need to see well at night generally have eyes with wide pupils. This optical strategy to improve photon capture may be improved neurally by summing the outputs of neighbouring visual channels (spatial summation) or by increasing the length of time a sample of photons is counted by the eye (temporal summation). These summation strategies only come at the cost of spatial and temporal resolution. A simple analytical model is developed to investigate whether the improved photon catch afforded by summation really improves vision in dim light, or whether the losses in resolution actually make vision worse. The model, developed for both vertebrate camera eyes and arthropod compound eyes, calculates the finest spatial detail perceivable by a given eye design at a specified light intensity and image velocity. Visual performance is calculated for the apposition compound eye of the locust, the superposition compound eye of the dung beetle and the camera eye of the nocturnal toad. The results reveal that spatial and temporal summation is extremely beneficial to vision in dim light, especially in small eyes (e.g. compound eyes), which have a restricted ability to collect photons optically. The model predicts that using optimum spatiotemporal summation the locust can extend its vision to light intensities more than 100 000 times dimmer than if it relied on its optics alone. The relative amounts of spatial and temporal summation predicted to be optimal in dim light depend on the image velocity. Animals which are sedentary and rely on seeing small, slow images (such as the toad) are predicted to rely more on temporal summation and less on spatial summation. The opposite strategy is predicted for animals which need to see large, fast images. The predictions of the model agree very well with the known visual behaviours of nocturnal animals.

Keywords: Spatial summation; Temporal summation; Spatial resolution; Temporal resolution; Sensitivity

1. Introduction

Seeing well in dim light is not a trivial task. For an eye adapted for vision on bright sunny days, a moonless night can be very dark indeed: light reaching the eye at midnight is typically 1000 million times dimmer than light reaching it at midday. Not surprisingly, maintaining peak visual performance over this huge range of intensity is impossible. Nevertheless, visual systems have at their disposal several optical and neural strategies which help to optimise visual performance over as wide a range of light intensities as possible. How these strategies optimise visual performance at night forms the basis of the present investigation.

The ability of a visual system to reliably detect visual information diminishes markedly with decreasing intensity. This is because the uncertainty associated with the random absorption of photons (which obeys Poisson statistics) is greater at lower intensity. If a photoreceptor absorbs a sample ('signal') of N photons during its integration time, the uncertainty ('noise') associated with this sample is $\sqrt{N}$. A useful measure of visual performance is the ratio of signal to noise (SNR) which in this simple case is $N/\sqrt{N}$, that is, $\sqrt{N}$ (see Snyder, 1979; Land, 1981). Thus SNR increases as the square root of photon absorption. Put another way, visual reliability improves with increasing light intensity. Despite its simplicity, this so-called Square-Root or de Vries–Rose law describes visual performance at low light levels quite well, both in vertebrates (reviewed by

* Corresponding author. Present address: Department of Zoology, University of Lund, Helgonavägen 3, S-22362 Lund, Sweden. Tel.: +46-46-222-9341; fax: +46-46-222-4425; e-mail: eric.warrant@zool.lu.se.

0042-6989/99/$ - see front matter
PII: S0042-6989(98)00262-4

Shapley & Enroth-Cugell, 1984; Hess, 1990; Sharpe, 1990) and invertebrates (Laughlin, 1981, 1990; Howard & Snyder, 1983). At higher light levels the square-root law breaks down due to adaptation (Barlow, 1965) and transduction saturation (Howard & Snyder, 1983). At extremely low light levels another factor limits reliability: spontaneous thermal activations of the phototransduction machinery, whose voltage waveforms are indistinguishable from those due to absorbed photons. This dark light (Barlow, 1956), present even in the absence of light, provides the ultimate limit to visual performance, as has elegantly been shown in amphibians (Aho, Donner, Hydén, Larsen & Reuter 1988; Aho, Donner, Helenius, Larsen & Reuter, 1993).

There are two possible ways for an eye to improve visual reliability in dim light: optically and neurally. Optically, a primarily diurnal eye can capture more light in dim conditions by widening its pupil or by increasing the angular subtense of its photoreceptors (by widening the photoreceptor (Williams, 1982, 1983), or shortening the focal length as found in a shrimp (Nilsson & Odselius, 1981)). Optical improvements rarely improve photon catch by more than a factor of 1000, which is far short of the 1000 million necessary. Much of this remaining shortfall can be met neurally. Firstly, at the level of the photoreceptors, the response gain (response per unit stimulus) can be increased with decreasing light intensity. Whilst not improving photon catch per se, increased gain in dim light can improve sensitivity by a further factor of 10–1000 (Laughlin, 1981; Bryceson & McIntyre, 1983; Shapley & Enroth-Cugell, 1984; Roebroek & Stavenga, 1990; Laughlin, 1990; Warrant & McIntyre, 1990a). Secondly, photon catch can be dramatically improved by summing photons in space and time (Pirenne & Denton, 1952; Pirenne, 1967; Lythgoe, 1979; Snyder, 1979).

1.1. Spatial and temporal summation

Visual systems sample the world through a matrix of parallel visual channels, the density of which determines spatial resolution. In vertebrate camera eyes, these channels are specified by the matrix of retinal ganglion cells (reviewed by Hughes, 1977; Appendix A). In compound eyes, the channels are equivalent to the ommatidia (and their underlying neural cartridges). In dim light, photon capture could be dramatically improved by coupling channels together, instead of allowing each to collect in isolation. In this way each channel could collect photons over a wide visual angle, the spatial receptive field now being much larger. This spatial summation between channels could be mediated by one or more classes of laterally spreading neurons. Such lateral neurons are well known architectural elements of both the vertebrate and invertebrate visual systems. Of course, the price paid to improve photon catch by spatial summation is a simultaneous and unavoidable loss of spatial resolution.

Whilst the exact neural substrate for a spatial summation strategy is not generally known, behavioural studies and electrophysiological recordings from higher visual centres in both vertebrates and invertebrates indicate that it does occur (e.g. Dvorak & Snyder, 1978; Pick & Buchner, 1979; Srinivasan & Dvorak, 1980; Dubs, Laughlin & Srinivasan, 1981; Dubs, 1982; Doujak, 1985; Schuling, Mastebroek, Bult & Lenting, 1989; De Valois & De Valois, 1990, pp. 196–203; Hallett, 1991, pp. 64–65; Nilsson & Ro, 1994). For example, in bright light the sampling grid of motion-correlating channels in the fly compound eye is equivalent to the grid of ommatidia. However, as light intensity falls, the correlator grid coarsens, a phenomenon which implies spatial summation (Dvorak & Snyder, 1978; Pick & Buchner, 1979; Srinivasan & Dvorak, 1980; Schuling et al., 1989).

Photon catch can also be significantly improved in dim light by extending the time during which a sample of photons is counted by the visual system. This is analogous to lengthening the shutter time on a camera in dim light (Lythgoe, 1979): a brighter image is sampled by the retina, but the resolution of moving objects is significantly degraded. The eye's shutter time, or integration time, can be set by the speed of the transduction cascade in the photoreceptors. The long integration times found in nocturnal toad rods (about 1.5 s) and deep-sea mysid rhabdoms (160 ms, very long for an arthropod) have been interpreted as strategies for improving photon capture (Donner, 1987, 1989; Aho et al., 1993; Moeller & Case, 1994; Donner, Koskelainen, Djupsund & Hemilä, 1995; Moeller & Case, 1995). In humans, the integration time in dim light is around 0.1 s (Barlow, 1958). In some animals the integration time may even be set by a slower neural mechanism higher in the visual pathway (as in the optokinetic system of crabs: Nalbach, 1989).

It is well known in both vertebrates and invertebrates that spatial and temporal summation decreases dynamically with increasing light intensity, eventually ceasing to be active. This is quite evident in contrast sensitivity functions (CSFs) measured both psychophysically and electrophysiologically. In bright light the spatial and temporal CSFs are band-pass in nature, accentuating middle-to-high spatial and temporal frequencies while suppressing low frequencies (reviewed by De Valois & De Valois, 1990). In the space and time domains this band-pass behaviour is equivalent to lateral inhibition and self inhibition, respectively both considered instrumental in reducing the large amount of redundant information inherent in natural scenes (Srinivasan, Laughlin & Dubs, 1982; Atick & Redlich, 1992), sharpening spatiotemporal contrasts (van Hateren, 1992a) and maximising the information capacity of early vision

Table 1
Glossary of symbols with species-specific ocular values[a]

Symbol	Meaning	Units	Beetle	Locust	Toad
Constants					
$\Delta\phi$	Angle between neighbouring input visual channels	deg	2.5	1.1	0.95
$\Delta\rho$	Half-width of input visual channel receptive field	deg	4.0	4.0	2.61
k	Absorption coefficient of the photoreceptor	μm^{-1}	0.0067	0.0067	0.035
κ	Quantum efficiency of transduction	–	0.5	0.5	0.34
ω	Specific dark variance	equiv. phot. μm^{-3} s^{-1}	1.3×10^{-6}	1.3×10^{-6}	6×10^{-5}
d	Photoreceptor diameter	μm	14	4.0	7.4
l	Photoreceptor length	μm	86	290	45
δ	Rod density in the retina	rods deg^{-2}	–	–	194
f	Focal length	μm	352	160	4200
A	Diameter of aperture (vertebrate pupil, insect facet lens)	μm	37	37	3007
τ	Transmission of the eye's optics	–	0.80	0.80	0.91
n_f	No. of facets contributing light to an input channel (insects only)	–	180	1	–
m	Mean contrast of the scene	–	0.5	0.5	0.5
Variables					
N	No. photons captured by an input channel in one integration time	photons			
I	Ambient light intensity	phot. μm^{-2} s^{-1} sr^{-1}			
σ_D^2	Total dark variance	Equivalent photons			
$\Delta\rho_p$	Half-width of spatial summation function	deg			
$\Delta\rho_T$	Half-width of receptive field of output visual channel	deg			
v	Image velocity	deg s^{-1}			
Δt	Integration time	s			
ν	Spatial frequency	c deg^{-1}			
ν_{max}	Maximum detectable spatial frequency	c deg^{-1}			

[a] Data from various sources: dung beetles (Warrant & McIntyre, 1990a,b), locusts (Wilson, 1975; Lillywhite, 1977; Wilson, Garrard & McGuinness, 1978; Williams, 1982; Laughlin & Lillywhite, 1982; Williams, 1983), toads (Aho et al., 1988, 1993). Values of k from Warrant and Nilsson, 1998. Locust values of ω and κ were used for dung beetles. $\Delta\rho$ in insects is the rhabdom acceptance angle, in toads it is 2/3 the angular size of the ganglion cell receptive field (empirically, from Donner & Grönholm, 1984). $\Delta\phi$ in toads is the inter-ganglion-cell angle, in insects it is the interommatidial angle.

(van Hateren, 1992a,b,c, 1993a,b,c). In dim light, when photon noise becomes limiting, spatial and temporal CSFs become low-pass in nature and high frequency information is lost. In the space and time domains this low-pass behaviour is equivalent to spatial and temporal summation respectively (van Hateren, 1992a). The way information acquisition in early vision is optimised during the transition from inhibition in bright light to summation in dim light, is beautifully treated by van Hateren, (van Hateren, 1992a,b,c, 1993a,b,c).

1.2. Does spatial and temporal summation help animals see better at night?

Even though the phenomenon of visual summation has been known for many years, its benefits (or otherwise) for animals with various eye designs and lifestyles have never been quantitatively investigated. In particular, can a strategy of spatial and temporal summation really help animals see better at night? Or do the unavoidable losses in resolution outweigh the gains in photon capture and actually make vision worse? To answer this question, I have developed a simple theoretical model derived from the well known model of Snyder (1977) and Snyder, Laughlin and Stavenga, (1977a,b). Using physiological, optical and anatomical data from insects and amphibians, and incorporating the effects of summation and dark noise, the model overwhelmingly indicates that spatial and temporal summation is immensely beneficial to vision at night, but that their relative contributions depend very much on the eye design and lifestyle of the nocturnally-active animal in question.

2. Theory

2.1. Animals modelled

I have chosen to model the eyes of three species: the camera eyes of the nocturnal toad *Bufo bufo*, the apposition compound eyes of the diurnal locust *Locusta migratoria* and the superposition compound eyes of the crepuscular dung beetle *Onitis alexis*. The optical, anatomical and physiological parameters necessary for the model are well known in these species, and values from the literature are given in Table 1.

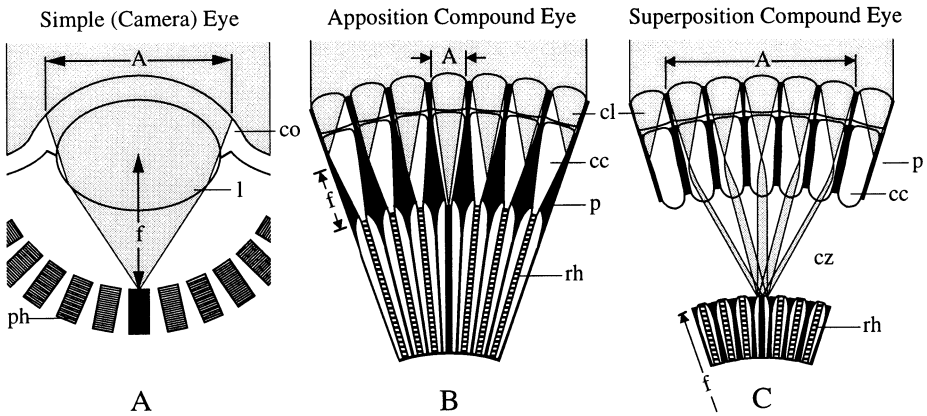

Fig. 1. Eye designs. (A) Simple (camera) eye. (B) Apposition compound eye. (C) Superposition compound eye. The paths and fates of parallel light rays, incident on the external eye surface, are indicated in each (shaded area). For each design the target photoreceptor is shaded black. *A* is the diameter of the aperture, *f* is the focal length (which in superposition eyes is measured from the eye's centre of curvature (not indicated)), *cl* is the corneal facet lens, *cc* is the crystalline cones, *co* is the cornea, *p* is the screening pigment, *rh* is the rhabdom, *ph* is the photoreceptor, *cz* is the clear zone, and *l* is the lens.

Toads are very sedentary animals which sit and wait in darkness for small slowly moving arthropods to crawl by. After visually tracking them, they shoot out their long sticky tongues to snap them up (Larsen & Pedersen, 1982; Aho et al., 1993). Toads, like all vertebrates, possess camera-type simple eyes (Fig. 1A), in which light is focused on the retina by a large single lens and (in terrestrial animals) an overlying cornea. This design can also be found in many invertebrates, including spiders and molluscs (Land, 1981; Nilsson, 1989).

Locusts and dung beetles are flying insects which use their eyes for orientation, and like all insects they possess compound eyes (Fig. 1B, C). Compound eyes are constructed of many individual optical elements called ommatidia, each of which contains one or two lenses which focus light onto an underlying photoreceptor (or rhabdom). Locusts have apposition compound eyes (Fig. 1B). In this design each ommatidium is isolated from its neighbours by a shroud of dense black pigment, thus ensuring that the rhabdom only receives light from the narrow field of view defined by its own small lens. Apposition eyes tend to have limited photon capturing ability (because of their small lens diameters; *A* in Fig. 1), but usually have better spatial resolution (they generally have thinner rhabdoms, better image quality and denser ommatidial packing). This design is therefore typical of insects active in bright light (e.g. flies, bees and dragonflies). Nevertheless, locusts are active at all times; flying, feeding and copulating during the day, and making long migration flights at night (Chapman, 1980).

Dung beetles like *Onitis* are active only in dim light. They emerge from underground hiding places well after sun-set and then fly off in search of new dung in which they feed, mate and lay eggs. Their superposition eyes (Fig. 1C) are typical of nocturnal insects, including various types of moths and beetles. In this design, the retina and lenses have been separated by a wide clear zone, and in addition they possess a large light-hungry aperture. Light from each direction is then focused preferentially onto single wide rhabdoms in the retina. The price paid by nocturnal superposition eyes for their improved photon capture is frequently a loss in spatial resolution, due to their wider rhabdoms, lower image quality and coarser ommatidial packing (Warrant & McIntyre, 1990b, 1991, 1992, 1993).

2.2. Signal, noise and spatial resolution

Consider an eye viewing a scene of mean contrast *m* (taken as 0.5) and mean luminance *I* (Fig. 2A). For theoretical simplicity, the scene is a sinusoidal striped grating with a stripe density defined by the spatial frequency *v* (c deg^{-1}): higher spatial frequencies indicate denser stripes and finer spatial detail (Fig. 2B). Light from the scene passes the pupil of the eye and is focused as an image on the retina. Each visual channel collects a sample of *N* photons from this image during each of its integration times Δt. The number of photons sampled not only depends on the amount of light reaching the retina, but also on the amount of this light which can be captured by the receptive field of the visual channel: wider receptive fields ($\Delta\rho_T$) capture more light. The number of photons *N* is simply the product of the light intensity *I*, the area of the pupil, the integration time Δt, the solid angular subtense of the channel, and the fraction of light incident on the channel which is absorbed for vision. Even though a wider receptive field captures more light, it also degrades spatial resolution: the finer spatial frequencies transmitted by the optics are gradually lost as the

receptive field widens. This effect is summarised by the modulation transfer function (MTF) of the eye, which shows the *potential* range of spatial frequencies visible to the eye. The MTF is simply the Fourier transform of the receptive field (Dubs, 1982; Warrant & McIntyre, 1993): wider receptive fields lead to narrower MTFs (narrower ranges of visible spatial frequencies).

These ideas have been elegantly summarised by Snyder, Laughlin and Stavenga (1977a,b) in a theory of eye design which calculates the signal and associated noise generated in channels by an image. I have built on this theory to include the effects of spatial and temporal summation and also the effects of dark noise. In addition, my treatment is a single-channel analysis of signal and noise and assumes that an adequate sampling array of channels is already present. The resolution of an eye is always set by the resolution of each of its visual channels. It is the response of individual channels which is modulated by a moving image, and the reliability of this modulation (and thus whether the eye can see it) depends intimately on the relative quantities of signal and noise generated in each channel (and not on their sampling array).

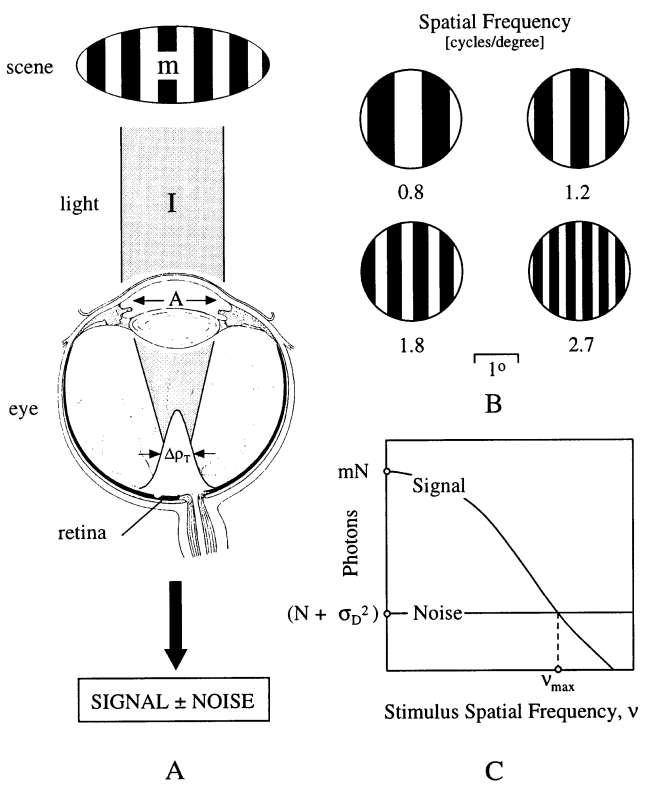

Fig. 2. Signal and noise in an eye. (A) The factors influencing signal and noise in an eye. If an eye is viewing a grating scene of spatial frequency v, contrast m and mean intensity I, the size of its aperture (A) determines the quantity of light focused on the retina. The receptive field of each channel (with half-width $\Delta\rho_T$) is due to the velocity of the image, the properties of the retina and the extent of spatial and temporal summation. (B) An explanation of spatial frequency with square gratings of increasing spatial frequency (c deg^{-1}). (C). Schematic graphs of signal and noise (Eqs. (1) and (3)). v_{max} is the maximum spatial frequency detectable by the eye, that is, the spatial frequency at which signal and noise become equal (found at the intersection of the signal and noise curves). N is the number of photons absorbed by the photoreceptor during its integration time, σ_D^2 is the total dark variance and m is the contrast of the scene.

The original theory also assumes that the spatial frequency power spectrum of the natural world is flat, but recent work has shown that the spectrum actually falls as v^{-2} (Field, 1987; van Hateren, 1992a). However, for the restricted range of lower spatial frequencies visible to insects, or to animals at night, the spectrum is effectively flat. The situation is rather different for a highly resolving eye in bright daylight (Laughlin, 1992).

The signal generated in a single visual channel when a pattern of spatial frequency v moves through its receptive field, is given by (Snyder et al., 1977a,b; Snyder, 1979):

$$\text{Signal} = m\ N\ M_T\ (v), \tag{1}$$

where $M_T\ (v)$ is the MTF, given by

$$M_T\ (v) = \exp\ [-3.56\ (v\ \Delta\rho_T)^2], \tag{2}$$

where $\Delta\rho_T$ is the half-width of the channel receptive field in degrees (Fig. 2A). This receptive field (and thus also its MTF) is taken as Gaussian for simplicity (see below).

The noise associated with the signal at low light levels is assumed to derive from two main sources: (1) photon shot noise ($\propto \sqrt{N}$) caused by the uncertainty associated with the random arrival of photons, and (2) dark noise associated with random thermal isomerisations of the photoreceptive membrane. The minor contribution from transducer noise and synaptic noise is neglected for simplicity. To account for dark noise we can consider each unit volume (μm^3) of a photoreceptor as an independent noise generator producing a signal variance ω per second. This is the specific dark variance, due to dark bumps and continuous voltage fluctuations. The total dark variance, σ_D^2, is simply $\omega V \Delta t$, where V is the total photoreceptive volume contributing to a visual channel. The total noise becomes (Donner, 1992):

$$\text{Noise} = \sqrt{(N + \sigma_D^2)}. \tag{3}$$

Signal and noise are plotted together schematically in Fig. 2C. The noise is independent of spatial frequency v, but via the MTF the signal is strongly dependent on v. A useful criterion for visual performance is the finest spatial frequency that can be resolved for a given photon catch and receptive field width. This can be conveniently defined as the spatial frequency at which the signal-to-noise ratio drops below one, which is equivalent to the point where the signal curve crosses the noise line in Fig. 2C. This is the maximum detectable spatial frequency, v_{max} (Warrant & McIntyre, 1993), and by equating Eqs. (1) and (3) we find

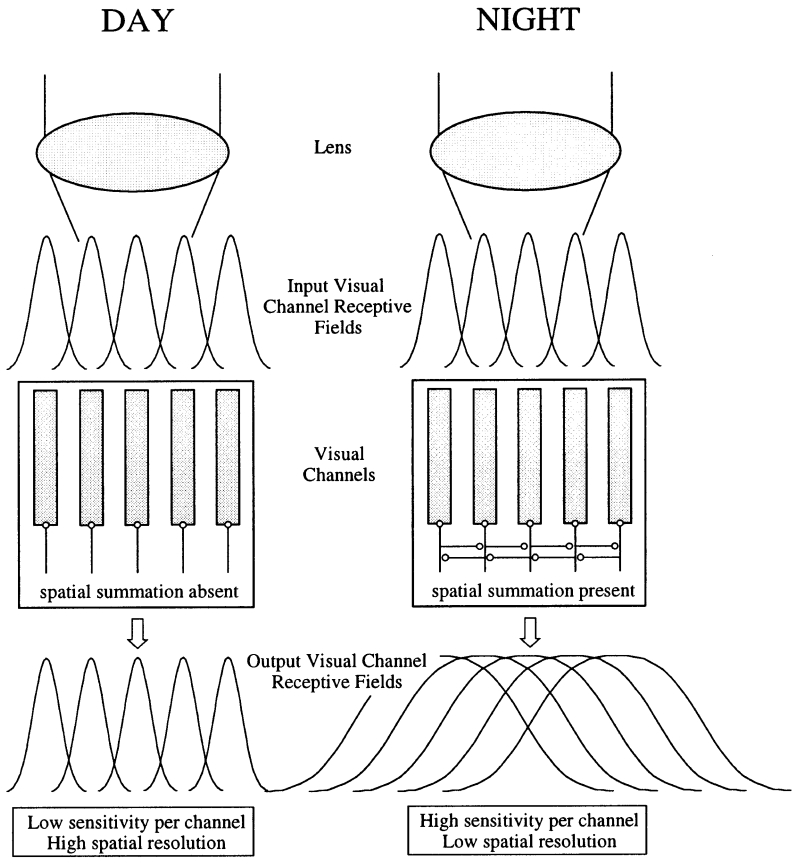

Fig. 3. Spatial summation. Both during night and day, images are formed on an array of input visual channels. These are equivalent to the rhabdoms in compound eyes or the ganglion cells in vertebrate camera eyes. During the day (left), when light is plentiful, sensitivity is not required. Spatial summation is inactive and the channels are neurally uncoupled. The receptive fields of the output visual channels (the channels post-summation) are equivalent to those of the input channels and the highest possible spatial resolution is achieved. During the night (right), when light is scarce, the input channels become coupled, either by lateral neural connections between channels, or by summing their outputs to single cells with wide dendritic fields. Whilst the number of output channels remains the same, spatial summation results in very wide output channel receptive fields and poor spatial resolution.

$$v_{\max} = \frac{0.530}{\Delta\rho_T}\sqrt{\ln mN - \frac{1}{2}\ln\left[N + \sigma_D^2\right]}. \quad (4)$$

I have used Eq. (4) to determine the optimum extent of spatial and temporal summation that an eye of given design should employ to maximise its value of $v_{\max}$ at different light intensities and for different image velocities. Eye design, summation, light intensity and image velocity all influence $v_{\max}$ via their effects on the values of N, $\Delta\rho_T$, and σ_D^2, expressions for which are given below.

2.3. Modelling spatial summation

Photon capture in dim light can be improved if signals from neighbouring channels are summed together (Fig. 3). Even though the original sampling matrix of visual channels remains intact, summation induces much wider receptive fields and thereby significantly degrades spatial resolution. This delicate tradeoff is tipped in favour of photon catch at lower light intensities, but as intensity increases and photons become more plentiful, the spatial extent of summation could be reduced (either continuously or in steps, depending on the neural circuitry underlying the summation), narrowing the receptive field of each channel and improving resolution (Pirenne & Denton, 1952; Pirenne, 1967; Lythgoe, 1979; Snyder, 1979). At daylight intensities, spatial summation could be turned off completely (Fig. 3), thereby providing maximum resolution.

In this study, a meaningful comparison between eye designs can only be made when the sampling matrix of input visual channels is defined by the matrix of ommatidia in compound eyes, and by the matrix of retinal ganglion cells in vertebrate camera eyes. The justification for this choice is that these are the matrices which are relevant to spatial resolution in the two eye types: regions of higher acuity (i.e. foveas) are defined by regions of higher ommatidial density in compound eyes (reviewed by Land, 1989), and higher ganglion cell density in vertebrate eyes (reviewed by Hughes, 1977). Of course the situation in vertebrate eyes is more

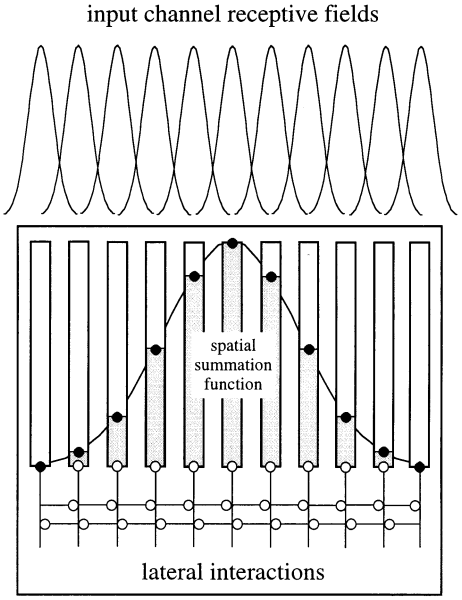

Fig. 4. The spatial summation function describes the strength of the lateral interactions between a visual channel (centre) and its neighbours. During spatial summation, coupling is strongest between nearest neighbours and gradually decreases with increasing distance from the channel (indicated by the area of hatching in each channel). In the model described here, the summation function is a three-dimensional Gaussian of half-width $\Delta\rho_p$ degrees.

complicated because of the complex cellular circuitry preceding the ganglion cells, and the fact that some ganglion cells receive inputs from single cones (e.g. P-ganglion cells the fovea), while others receive inputs from large pools of rods or cones (e.g. M-ganglion cells throughout the retina). Even though the size of the photoreceptor input sets the resolution (and sensitivity) of each ganglion cell, it is the ganglion cell matrix which is relevant for the type of spatial summation discussed here (see Appendix A for further details).

Each input visual channel (Fig. 3) supplies a signal which is proportional to the total photon catch N it receives in each integration time Δt, from the solid angle of visual space defined by its own (Gaussian) receptive field. In dim light, these signals could be laterally summed according to some spatial summation function (Fig. 4), which describes the strength of the lateral interactions responsible for summation. These interactions are assumed to weaken with distance from the central channel, with most summation deriving from nearer neighbours and less from those further away. The spatial summation function shown in Fig. 4 is a Gaussian, but much squarer functions might also be possible (implying more even summation with distance). Interestingly, in the early stages of this study I used numerical calculations and found only marginal improvements in visual performance for summation functions squarer than Gaussian. I therefore decided to use a simpler analytical model based solely on Gaussian receptive fields and summation functions.

The spatial summation function has a half-width of $\Delta\rho_p$ degrees (Fig. 5). As $\Delta\rho_p$ widens (as it might when light levels fall), the number of input channels (in two dimensions) which contribute to summation gets larger. This improvement in photon catch is offset by the loss of spatial resolution due to the wider receptive fields.

2.4. Modelling temporal summation

As we have mentioned, the integration time (Δt) is the time during which the visual system collects a sample of photons. This implies that a visual system with a longer integration time has a greater photon catch. An alternative view is that longer integration times reflect a temporal low-pass filtering operation on the incoming visual signal. This improves the signal-to-noise ratio by removing unwanted noise at high temporal frequencies (van Hateren, 1992a, 1993a). In reality both views are equivalent. For theoretical simplicity, I

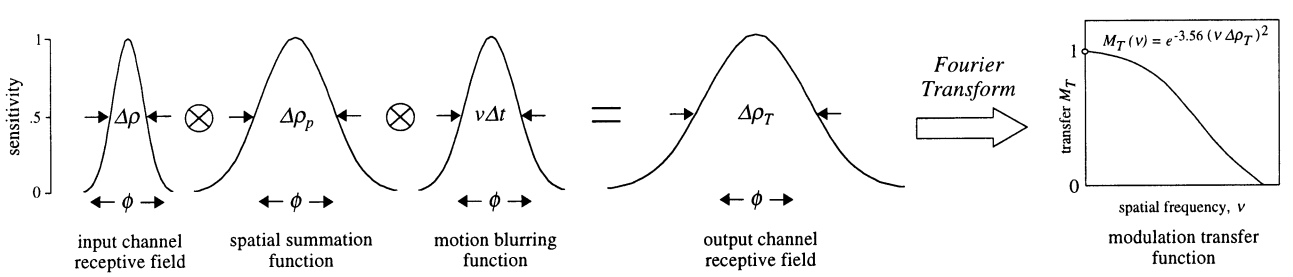

Fig. 5. A simple model of spatiotemporal summation. The receptive field of the output channel is determined by the receptive field of the input channel and the extent of spatial and temporal summation. The input channel receptive field is modelled as a Gaussian of half-width $\Delta\rho$ degrees. Temporal summation effects the spatial resolution of moving objects, which become spatially blurred by an amount $v\,\Delta t$ degrees, where v is the image velocity (deg s^{-1}) and Δt is the integration time (s). A motion blurring function can be modelled as a Gaussian of half-width $v\,\Delta t$ degrees. We can model the output receptive field as the convolutions of the input channel receptive field, the spatial summation function (Fig. 4) and the motion blurring function (circle-with-cross symbolises convolution). The output channel receptive field is a Gaussian of half-width $\Delta\rho_T$ degrees (given by Eq. (5)), whose Fourier transform yields the modulation transfer function $M_T(\nu)$ used to calculate the signal (Eqs. (1) and (2)). Originally the model was numerical and used an entirely different approach, and convolution was not assumed. After numerical evaluation it became apparent that the result obtained was identical to a convolution. The ϕ-axis is an angle axis in degrees.

will use the approach of Aho et al. 1993 and treat the integration time as the time in which the visual channel collects its sample of photons.

The disadvantage of a longer integration time is that it leads to poorer temporal resolution: objects moving quickly cannot be seen clearly. The length of the integration time effects the amount of spatial detail that can be perceived within a moving object, as well as its minimum size (Srinivasan & Bernard, 1975; Burr & Ross, 1982). The effects of integration time and image motion on spatial resolution can be modelled by a motion blurring function (Srinivasan & Bernard, 1975; Snyder, 1977), again assumed Gaussian for simplicity (Fig. 5). If an object moves with an angular velocity v deg s^{-1}, then during one integration time (Δt) its image is displaced an angular distance of $v\Delta t$ degrees across the retina. This additional spatial uncertainty associated with motion can be modelled with a motion blurring function of half-width $v\Delta t$. A fast image velocity and/or a long integration time results in a loss of spatial resolution via a widening of the motion blurring function.

2.5. A simple model of spatiotemporal summation

We are now in a position to account for the effects of spatiotemporal summation and image motion on the size of the receptive field of the output visual channel (Fig. 3). Following and extending Snyder's (1977) approach, I will simply model the output receptive field as the convolution of three Gaussian functions (Fig. 5): the receptive field of each input visual channel that contributes to summation (half-width $\Delta\rho$), the spatial summation function (half-width $\Delta\rho_p$) and the motion blurring function (half-width $v\Delta t$). Note that an input visual channel is equivalent to an ommatidium in compound eyes, and to a ganglion cell in vertebrate camera eyes. The output receptive field is also Gaussian with a half-width $\Delta\rho_T$ given by

$$\Delta\rho_T = \sqrt{\Delta\rho^2 + \Delta\rho_P^2 + (v\,\Delta t)^2}. \quad (5)$$

The MTF of the output visual channel is the Fourier transform of its receptive field (Fig. 5) and is specified by Eq. (2).

To calculate the maximum detectable spatial frequency v_{max} (Eq. (4)) we need expressions for N (the number of photons sampled by a visual channel during one integration time) and σ_D^2 (the total dark variance). These expressions depend on whether the eye being considered is a camera eye or a compound eye (see Appendix B).

Consider a compound eye of focal length f and interommatidial angle $\Delta\phi$ which uses n_f equally-contributing facet lenses of diameter A to focus light onto photoreceptors of length l and diameter d. In an apposition eye $n_f = 1$, while in a superposition eye it may be over 1000 (Warrant & McIntyre, 1996). We can show (see Appendix B):

$$N = 0.890\, n_f\, \kappa\tau \left(\frac{kl}{2.3+kl}\right) \Delta t \left(\frac{dA}{f}\right)^2 I \text{ (no summation)} \quad (6a)$$

$$= 1.269\, n_f\, \kappa\tau \left(\frac{kl}{2.3+kl}\right) \Delta t \left(\frac{\Delta\rho_P\, dA}{\Delta\phi\, f}\right)^2 I \text{ (summation)} \quad (6b)$$

and

$$\sigma_D^2 = 0.785\, \omega\, l\, \Delta t\, d^2 \text{ (no summation)} \quad (7a)$$

$$= 1.131\, \omega\, l\, \Delta t \left(\frac{\Delta\rho_P\, d}{\Delta\phi}\right)^2 \text{ (summation)} \quad (7b)$$

where k is the absorption coefficient of the photoreceptor (taken as 0.0067 for invertebrates and 0.035 μm^{-1} for vertebrates: see Warrant and Nilsson (1998) for values and references), κ is the quantum capture efficiency of the transduction process and τ is the fraction of incident light transmitted by the optics of the eye. For rod vision in camera eyes the expressions are similar except that $\Delta\phi$ now specifies the angle between the centres of visual fields of neighbouring ganglion cells, and $\Delta\rho$ the half-width of the ganglion cell receptive field (assumed Gaussian: see Donner & Grönholm, 1984; Copenhagen, Hemilä & Reuter, 1990). A is the diameter of the pupil. In order to account for the large pool of rods forming the receptive field of each ganglion cell (see Appendix A), we must also include the rod density in the retina δ (rods per deg^2):

$$N = 1.003\, \delta\, \kappa\tau \left(\frac{kl}{2.3+kl}\right) \Delta t\, \Delta\rho^2 \left(\frac{dA}{f}\right)^2 I$$

(no summation) (8a)

$$= 1.430\, \delta\, \kappa\tau \left(\frac{kl}{2.3+kl}\right) \Delta t\, \Delta\rho^2 \left(\frac{\Delta\rho_P\, dA}{\Delta\phi\, f}\right)^2 I$$

(summation) (8b)

and

$$\sigma_D^2 = 0.888\, \omega\, \delta\, l\, \Delta t\, \Delta\rho^2 d^2 \text{ (no summation)} \quad (9a)$$

$$= 1.269\, \omega\, \delta\, l\, \Delta t\, \Delta\rho^2 \left(\frac{\Delta\rho_P\, d}{\Delta\phi}\right)^2. \text{ (summation)} \quad (9b)$$

We now have everything we need to calculate v_{max} at different light intensities (I) and image velocities (v) for varying degrees of spatial summation ($\Delta\rho_p$) and temporal summation (Δt). These four parameters are the only variables in the model. All the other parameters are anatomical and physiological values specific to the eyes of the three species being modelled (Table 1). I will use Eqs. 4–9 and Table 1 to calculate the values

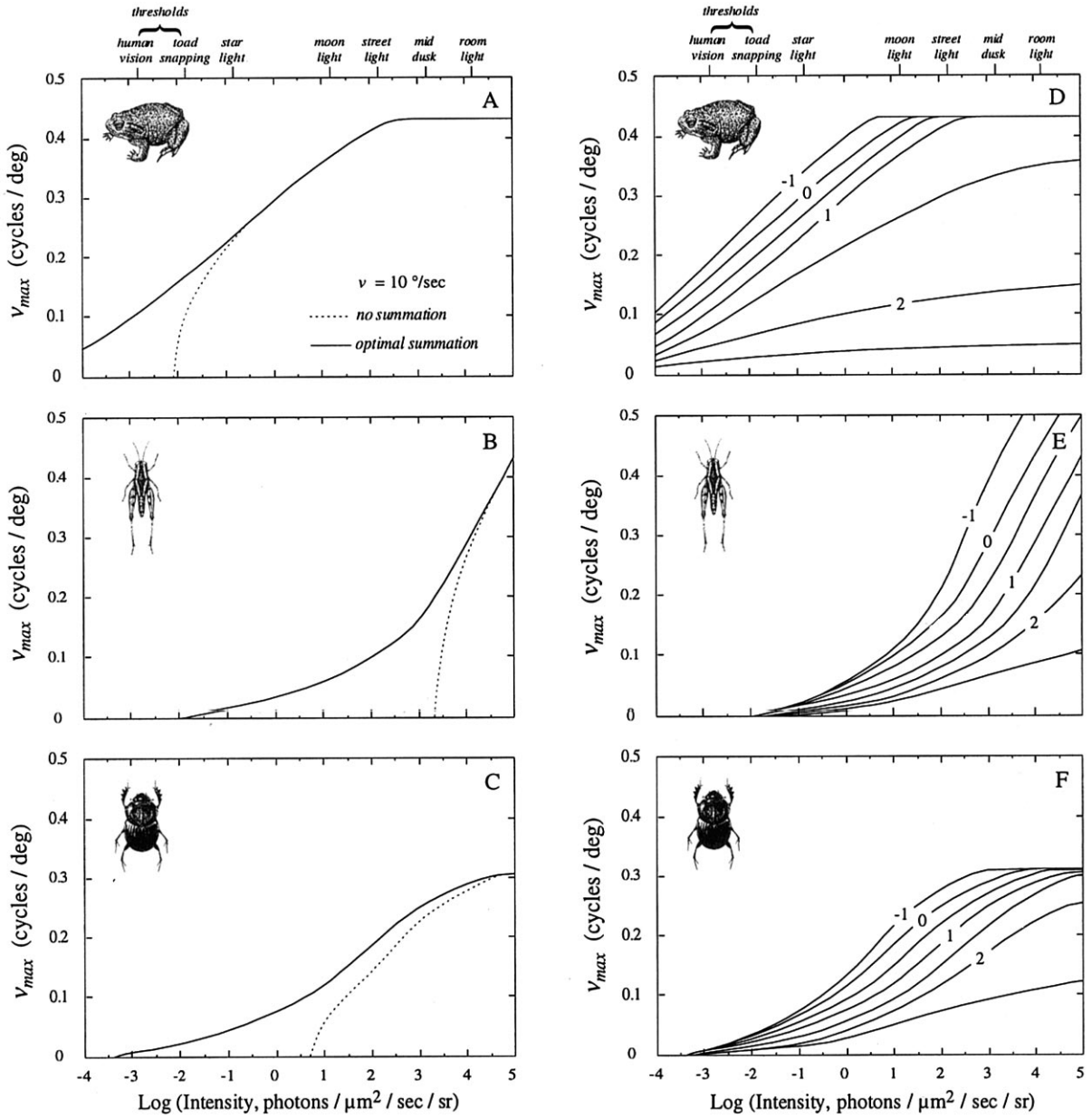

Fig. 6. Visual performance (as measured by the maximum detectable spatial frequency, v_{max}: Eq. (4)) at different light intensities and image velocities in the toad (A, D), the locust (B, E) and the dung beetle (C, F). At an image velocity of 10 deg s^{-1} (A–C), optimum spatial and temporal summation (solid line) extends vision to much lower light intensities (non-zero v_{max}) than if summation is absent and vision relies on the optics of the eye alone (dashed line). Vision in the locust is extended to starlight levels, whereas without summation the locust would become blind at mid-dusk. Faster images degrade visual performance (D–F) by lowering the highest attainable value of v_{max} (at any intensity). Curves in D–F are labelled in logarithmic units of image velocity (deg s^{-1}), in 0.5 log unit steps. Equivalent natural intensities are also shown. In the toad and the beetle v_{max} saturates at higher intensities for lower image velocities. This is because (in the model) v_{max} is not allowed to exceed the maximum spatial frequency passed by the receptive field of the input channel. This criterion maximum is defined as the spatial frequency at which the MTF of the receptive field falls to 1% of its maximum (simply given by 1.137 $\Delta\rho^{-1}$, where $\Delta\rho$ is the half-width of the receptive field in degrees). Note also that in this, and following figures, the real-world light intensity markers are derived from measurements of a half-clear sky during a 12 h period spanning midday to midnight. Light intensity measurements were made with a vertically oriented detector receiving a narrow cone of light filtered through a 550 ± 10 nm interference filter (see Warrant & McIntyre, 1992, Fig. 1). These values are approximately eight times lower than those obtained by assuming the wide spectral sensitivity curve of a standard human observer (centred at 555 nm: see Land, 1981, Table 3).

of $\Delta\rho_p$ (spatial summation) and Δt (temporal summation) which maximise v_{max} at each light intensity and image velocity. This allows us to explore the relative benefits of spatial and temporal summation for vision in dim light in animals with different eye designs and lifestyles.

3. Results

According to the model, animals which need to see well in dim light would benefit greatly from employing a strategy of spatiotemporal summation (Fig. 6A–C). In the absence of summation all three animals lose their ability to resolve spatial details in a scene (i.e. when $v_{max} = 0$) at a much higher intensity than when summation is activated optimally. Without summation locusts become blind at mid-dusk intensities, but with optimal summation locusts can extend their vision into starlight, which is over 5 log units dimmer (image velocity $v = 10$ deg s^{-1}: Fig. 6B). Thus, even though summation compromises both spatial and temporal resolution, this is far outweighed by the overall improvement in photon capture. Vision in dim light is thereby greatly improved.

The effects of image velocity on the optimum v_{max} are shown in Fig. 6D–F. For all animals, visual performance declines at all intensities with increasing image velocity (curves shown in Fig. 6D–F are for different v, in 0.5 log unit steps). This result agrees well with what is known about the effects of image motion on spatial resolution (Burr, 1991) and visual performance (van Hateren, 1993b).

According to the model, the toad has the best vision in dim light (Fig. 6A, D), followed by the dung beetle (Fig. 6C, F) and then by the locust (Fig. 6B, E). Each animal was given the same possibilities for spatial and temporal summation so the differences reflect the abilities of the different eyes to capture photons optically. The toad camera eye has a very wide pupil (3 mm) compared to the beetle superposition eye (0.5 mm) or the locust apposition eye (0.037 mm) and also uses a large pool of 750 rods to collect photons for each ganglion cell (Aho et al., 1993; see Appendix A). With these advantages the toad sees well in starlight even without summation between ganglion cells (Fig. 6A).

The optimum extent of spatial ($\Delta\rho_p$) and temporal (Δt) summation that gave the optimum v_{max} curves of Fig. 6D–F are shown in Fig. 7. In general, as light intensity falls, the optimum value of v_{max} is achieved by increasing extents of both spatial and temporal summation. In locusts, for example, $\Delta\rho_p$ rises slowly with decreasing light intensity, reaching values of between 4 and 15° (depending on v) in moonlight (Fig. 7B). Below this intensity the optimum $\Delta\rho_p$ sharply escalates. At any given intensity, larger values of $\Delta\rho_p$ are predicted to be optimal for higher image velocities (see also Fig. 8E). Temporally, the situation is similar: like $\Delta\rho_p$, Δt first rises slowly with decreasing light intensity, and then escalates (Fig. 7E). However, unlike $\Delta\rho_p$, Δt is predicted to be higher at a given light intensity for a smaller image velocity. There thus appears to be a trade-off between spatial and temporal summation which depends on the image velocities of interest to the animal. This point will be addressed shortly (Fig. 8).

At this point it is useful to say something about the tolerance in the value of v_{max} predicted to be optimal for a given light intensity and image velocity. Even though the calculation finds the highest value of v_{max} (and corresponding values of $\Delta\rho_p$ and Δt), it is possible that v_{max} does not decline significantly at other values of $\Delta\rho_p$ and Δt near their optimum values. To test this, consider the locust at Log $I = 1$ and $v = 10$ deg s^{-1}. The highest value of v_{max} is predicted when $\Delta\rho_p = 8.8°$ and $\Delta t = 600$ ms. However, values of v_{max} that are 90% of maximum or greater occur for $\Delta\rho_p$ between 6.3 and 13.5° and Δt between 350 and 1080 ms. Thus, there is quite a good tolerance in the extents of spatial and temporal summation necessary to give a near-maximum value of v_{max}. This means that the balance between $\Delta\rho_p$ and Δt can be manipulated in a particular animal without compromising visual performance too badly (e.g. to improve some other aspect of vision). The actual values of $\Delta\rho_p$ and Δt possessed by an animal may therefore differ slightly from the predicted values.

Many of the important principles of optimum spatiotemporal summation become clear if we hold image velocity constant ($v = 10$ deg s^{-1}) and vary light intensity (Fig. 8A–C) or hold light intensity constant (Log $I = 0$) and vary image velocity (Fig. 8D–F). At constant image velocity, we again see that both spatial and temporal summation are predicted to increase with decreasing light intensity. Exactly how much spatial and temporal summation is optimum at a given light intensity depends on the eye design: a design which captures more light optically depends less on summation. In starlight, the wide-pupil toad eye (Fig. 8A) has barely begun to sum ($\Delta\rho_p = 1°$; $\Delta t = 0.1$ s), the beetle superposition eye (Fig. 8C) is summing moderately ($\Delta\rho_p = 8°$; $\Delta t = 0.5$ s) while the locust apposition eye (Fig. 8C) is summing heavily ($\Delta\rho_p = 22°$; $\Delta t = 1.8$ s). Eye design is also reflected in the light intensity at which spatial and temporal summation is 'turned on' in the three different eyes. We can say that spatial summation turns on as soon as $\Delta\rho_p$ is predicted to be nonzero. Temporal summation turns on when Δt rises above the normal light adapted value (100 ms in toads, 25 ms in beetles and locusts). Spatial summation turns on in moonlight in toads, at mid-dusk in beetles and at early dusk in locusts. Temporal summation turns on in starlight in toads, in room light in beetles and at early dusk in locusts. Again, if an eye can capture more light optically, it can afford to rely less upon summation.

At a constant light intensity (Log $I = 0$), the trade-off between spatial and temporal summation at different image velocities is immediately evident (Fig. 8D–F). As image velocity increases, the optimum strategy of summation involves more spatial summation and less tem-

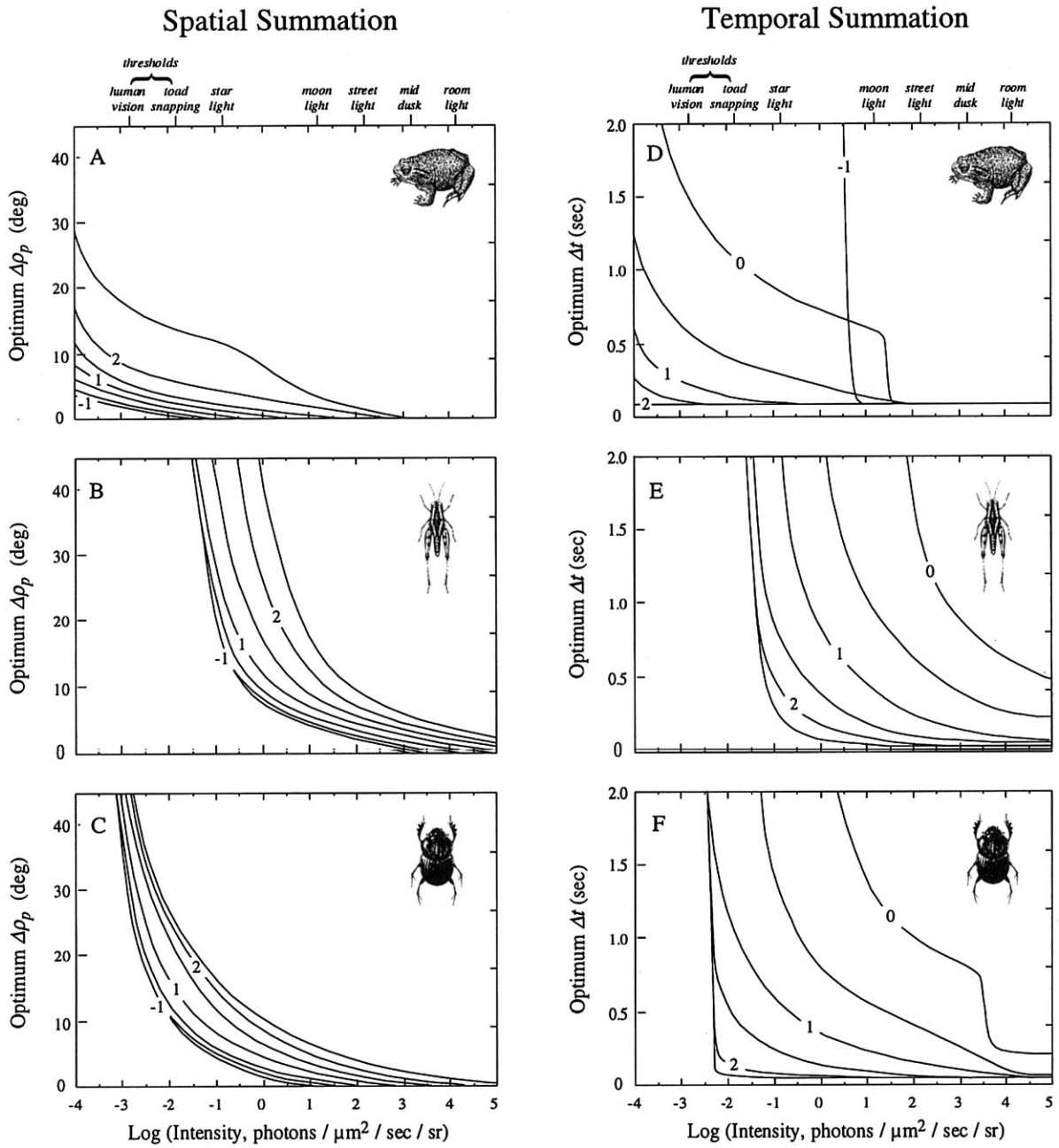

Fig. 7. The optimum spatial (A–C) and temporal (D–F) summation that led to the curves of Fig. 6D–F, as a function of light intensity and image velocity in the toad (A, D), the locust (B, E) and the dung beetle (C, F). Again, curves are labelled in logarithmic units of image velocity (deg s^{-1}), in 0.5 log unit steps. Equivalent natural intensities are also shown. The extents of both spatial summation ($\Delta\rho_p$) and temporal summation (Δt) are expected to rise with decreasing light level, the rises being greatest and occurring earliest in the locust apposition eye, followed by the beetle superposition eye and finally by the toad camera eye. Eyes which gather a lot of light optically (such as those of the toad) need to rely less on summation to see well in dim light. The 'cliff-edge' temporal summation curves evident at low image velocities in toads and beetles are due to the saturation of v_{max} explained in Fig. 6 (caption).

poral summation. This is intuitively easy to understand because if the animal needs to see objects (albeit large ones!) moving quickly in dim light, then the best way to collect sufficient photons is to maintain good temporal resolution and use spatial summation instead. The opposite is true for animals which need to see small, slowly moving objects. In this case it would be better to maintain good spatial resolution and use temporal summation to collect photons.

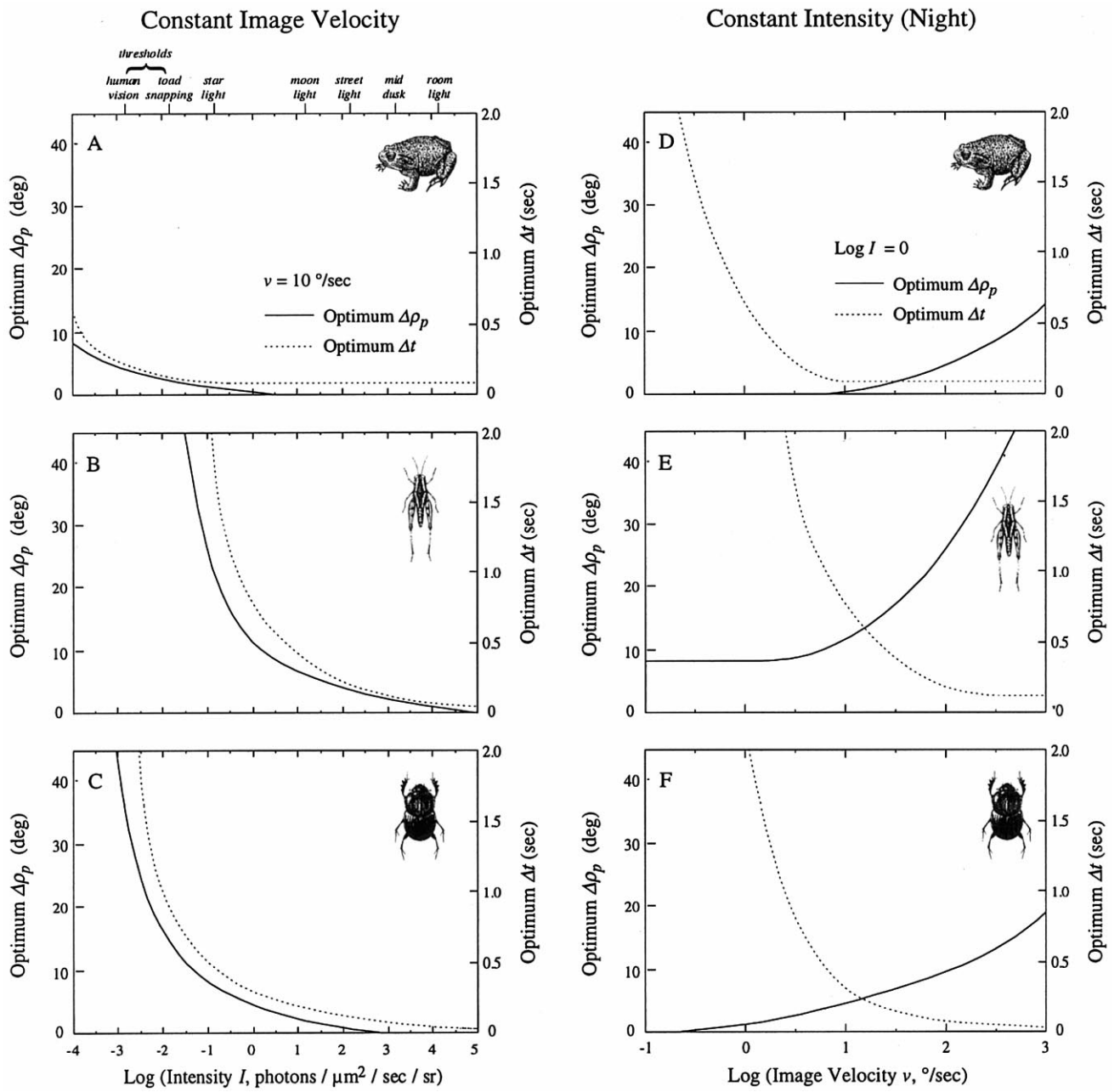

Fig. 8. The optimum spatial summation ($\Delta\rho_p$, solid lines) and temporal summation (Δt, dashed lines) as a function of light intensity at constant image velocity (10 deg s^{-1}: A–C), and as a function of image velocity at constant light intensity (Log $I = 0$ (night): D–F). Curves are shown for the toad (A, D), the locust (B, E) and the dung beetle (C, F). At constant image velocity both spatial and temporal summation are predicted to rise with decreasing light intensity (data from Fig. 7). At constant light intensity there is a trade-off between spatial and temporal summation with image velocity. At lower velocities temporal summation is predicted to dominate, whereas at higher velocities spatial summation is predicted to dominate.

4. Discussion

Can spatial and temporal summation help animals see better at night? This, the central question of the present investigation, is easily answered. Despite the unavoidable compromise in spatial and temporal resolution, the vastly enhanced photon catch afforded by visual summation significantly improves visual performance in dim light (Fig. 6). Visual performance is readily quantified as a single parameter, the maximum detectable spatial frequency v_{max}, which specifies the finest spatial detail which a visual system can resolve at any given light intensity and image velocity. This parameter quantifies the trade-off between resolution and photon capture made in an eye attempting to see a dim, moving image contaminated by shot noise and dark noise. Using a simple model to calculate v_{max}, it has been possible to predict many features of optimum

spatiotemporal summation and how they relate to the eye designs and lifestyles of different animals.

4.1. Summation and eye design

In the three eyes I have compared (the camera eye of the nocturnal toad, the apposition eye of the locust and the superposition eye of the beetle), clear patterns emerge. The first is that an eye will always perform better in dim light if it can collect as many photons as possible optically and thereby minimise dependence on spatial and temporal summation. Eyes like those in the toad, with larger pupils, will always perform better in dim light. Compared to insects, toads also have another advantage: their eyes, like those of all vertebrates, possess pools of rods which sum their signals to provide input to the ganglion cells. In dim light, these pools can contain up to 1000 rods (Aho et al., 1993) thereby providing an initial hard-wired spatial summation (Appendix A). The good photon catch provided by a wide pupil and extensive rod pooling may diminish the need for a second spatial summation between ganglion cells, and this certainly seems to be the prediction of the model (Figs. 6A and 8A). It is therefore quite possible that nocturnal vertebrates rely more upon optical and retinal strategies for vision in dim light.

Apposition eyes, on the other hand, are much smaller and have limited pupil sizes. In addition, each channel only has access to photons collected by a single facet (the neural superposition eyes of higher flies are an exception, providing a signal which has been pooled from rhabdomeres under six facets). The model predicts that spatial and temporal summation are likely to be much more useful in these smaller eyes.

Animals like locusts, which have to see well in a wide range of light intensities, clearly face difficulties. Their apposition compound eye is the typical design for day-active insects, and because of the small ommatidial pupil it is an inherently unsuitable design for night vision. Nevertheless, locusts need to see at night, and apart from a night-time widening of the photoreceptors (Williams, 1982, 1983), spatiotemporal summation is the only remaining strategy. Certainly, if activated optimally, summation has the potential to drastically improve the locust's visual performance at night, extending vision to intensities 100 000 times dimmer (Fig. 6B). Summation can therefore turn a diurnal eye into a passable nocturnal eye. Recent work indicates that this actually seems to be the case in bees, which see better in dim light than their apposition eyes should allow, thus explaining how tropical bees and wasps can forage at night (Warrant, Porombka & Kirchner, 1996). Summation has such obvious benefits that it is likely to be widespread in nature.

Clearly, the best compound eye design for vision at night is the superposition design. The wide pupils of superposition eyes allow them to collect much more light than an apposition eye of similar size, and this, coupled to spatial and temporal summation, gives the potential for much better nocturnal visual performance, especially during flight.

4.2. Summation, image motion and lifestyle

An animal that needs to see moving images (due to its own-self motion or to the motion of external objects in the visual field) may have problems doing so in dim light. If the animal relies on a longer integration time to improve photon capture, this will have serious consequences for the perception of motion. Any person familiar with photography will know that increasing the shutter time on a camera in dim light can result in 'smeared' images of moving objects. Whilst our visual system rarely perceives the motion of objects as smeared (Burr, 1980), the length of our integration time does effect the amount of spatial detail we can perceive within a moving object, as well as its minimum perceivable size (Srinivasan & Bernard, 1975; Burr & Ross, 1982). In other words, good temporal resolution of a moving object is only maintained at the expense of its spatial resolution. When light levels fall and our integration time lengthens to capture more photons, we can only see fast-moving objects if they are large, and small objects only if they are relatively slow (reviewed by Burr, 1991). Even then we may still have difficulty discerning spatial details of the objects internal structure (for a lovely photographic demonstration of this see Lythgoe (1979), Fig. 2.32).

Not surprisingly then, the model predicts that visual performance in dim light strongly depends on image velocity (Fig. 8D, E, F). An animal wishing to resolve faster images should improve photon catch by employing spatial summation rather than temporal summation. Such a strategy maintains good temporal resolution, but sacrifices spatial resolution. This allows the perception of larger fast-moving objects, but not smaller ones (smaller objects require better spatial resolution). Locusts and other insects (like beetles and moths) which fly at night encounter high image velocities. Collection of flow-field information in dim light during flight may best be subserved by a strategy of spatial (rather than temporal) summation. Even though the finer spatial details of the flow field will be lost, rapid changes in the grosser features (which are still sufficient for flow-field analysis) will be preserved.

The opposite strategy is predicted for animals trying to see small, slowly moving images: photon capture should occur via temporal rather than spatial summation. It is quite possible that this is the strategy nocturnal toads use to detect small, slowly moving wood lice. Their very long integration times (up to 1.6 s) seem well adapted for such a strategy, and would be ideal for

detecting these arthropods (Aho et al., 1993). The model predicts that a toad viewing a wood louse moving at 1 deg s^{-1} should not use spatial summation but instead sum temporally with an integration time of 0.75 s (Fig. 8D). Whilst this is only half the integration time toads actually have, the theory nevertheless predicts approximately the right visual strategy for this eye design. At the threshold of toad snapping behaviour the model predicts an integration time of 1.1 s. Certain species of crabs provide an even more extreme example. Doujak (1985) found that the crab *Leptograpsus* can track dim point sources of light moving at only 180 deg h^{-1} (0.05 deg s^{-1}). Other crabs are even known to track movements as slow as 15 deg h^{-1} (Horridge & Sandeman, 1964; Sandeman & Erber, 1976). This ability in crabs would be best served exclusively by a strategy of temporal summation. At any rate, spatial summation is useless for improving discrimination of point sources. A trade-off between spatial and temporal resolution with image velocity has also been inferred in a recent study of optimum spatiotemporal filtering in early vision (van Hateren, 1993b).

From the above discussion, one thing seems quite clear from the model: the strategy of spatiotemporal summation adopted by an animal in dim light produces a visual filter that selects moving objects of a particular size and speed. In the case of the toad, the filter should be optimally sensitive to those features of the world which are of greatest interest to toads: small, slowly moving wood lice. For another animal, the filter may be set to optimally detect larger, faster objects. As far as I know, this important aspect of nocturnal visual ecology has never been investigated.

Finally, the vertebrate visual system has one very important advantage over its invertebrate counterpart with respect to image motion. Vertebrate eyes can move, and thereby track moving objects. Tracking a moving object reduces the relative velocity between the object and the eye, and this greatly improves the perception of the object (as elegantly shown by Eckert & Buchsbaum, 1993). Even though lacking eye movements, some invertebrates can still reap the benefits of tracking moving objects. Flying insects, like flies and dragonflies, chase (i.e. track) other insects by attempting to hold them within the foveal field of view (reviewed by Wehner, 1981). Mantids, agile stalking hunters, have the rare ability among insects to track moving targets (i.e. prey) by turning the entire head.

One may therefore expect that the strategy of summation adopted by an animal reflects its lifestyle. Of course, animals may have varied behaviour and may need to rely on vision for both fast and slow image analysis. In this case, parallel visual channels with different balances between spatial and temporal summation may subserve these different behaviours. Parallel fast and slow motion pathways have been postulated in both vertebrates (Kulikowski & Tolhurst, 1973; Tolhurst, 1973; Murray, Macana & Kulikowski, 1983) and invertebrates (Nalbach, 1989; Horridge & Marcelja, 1992). Alternatively, different parts of the visual field (or in spiders, even entirely different eyes) might be used for different spatio–temporal tasks.

4.3. The possible neural basis of spatial summation

Now that we have established the benefits of spatial summation, how might it be subserved neurally? Several schemes have been proposed (Pirenne & Denton, 1952; Pirenne, 1967; Srinivasan & Dvorak, 1980). The two most plausible alternatives are shown in Fig. 9.

The first scheme involves the inter-connection of visual channels by a class (or classes) of cells with widely spreading lateral fibres (Fig. 9A). As an example of the kinds of cells which might be involved, we can consider the insect lamina. This neuropil contains a cartridge of neurons underlying each ommatidium. Each cartridge contains two kinds of neurons: (1) *throughput* neurons (such as the LMC (monopolar) cells) which carry information from each ommatidium through the lamina to the next neuropil, the medulla, and (2) *lateral* neurons (such as amacrine and tangential cells), which inter-connect the throughput neurons over as many as 40 cartridges (Strausfeld & Campos-Ortega, 1977). In bright light, the lateral neurons have been postulated to subserve lateral inhibition in the LMC pathway (Strausfeld & Campos-Ortega, 1977; Strausfeld, 1989; Yang, 1994), although lateral inhibition may also be caused by the extracellular field potential of the lamina (Shaw, 1984). In dim light the lateral interaction may change from inhibition to summation (Dubs et al., 1981), and the extent of the lateral summation may widen with decreasing light intensity (describable by a spatial summation function, like the one in Fig. 4). Such a scheme might explain the larger-than-expected LMC response to dim, wide-field illumination in the dark adapted fly lamina (Dubs et al., 1981). Light-dependent changes in lateral interactions are still hypothetical and require substantial plasticity in the synaptology of the amacrine and tangential cell circuits thought to be involved. However, such plasticity in peripheral visual circuitry is well-known (e.g. Raynauld, Laviolette & Wagner, 1979; Weiler, Kohler, Kirsch & Wagner, 1988), and in some cases is even controlled by a circadian rhythm (Pyza & Meinertzhagen, 1993).

The second scheme involves single cells, each of which has a wide dendritic field spatially summing the outputs of the visual channels (Fig. 9B). These cells could form classes, each class having a certain dendritic field size subserving a different extent of spatial summation. Each point in space could then be represented by several cell classes, ranging from those with smallest dendritic field (least summation and best resolution) up

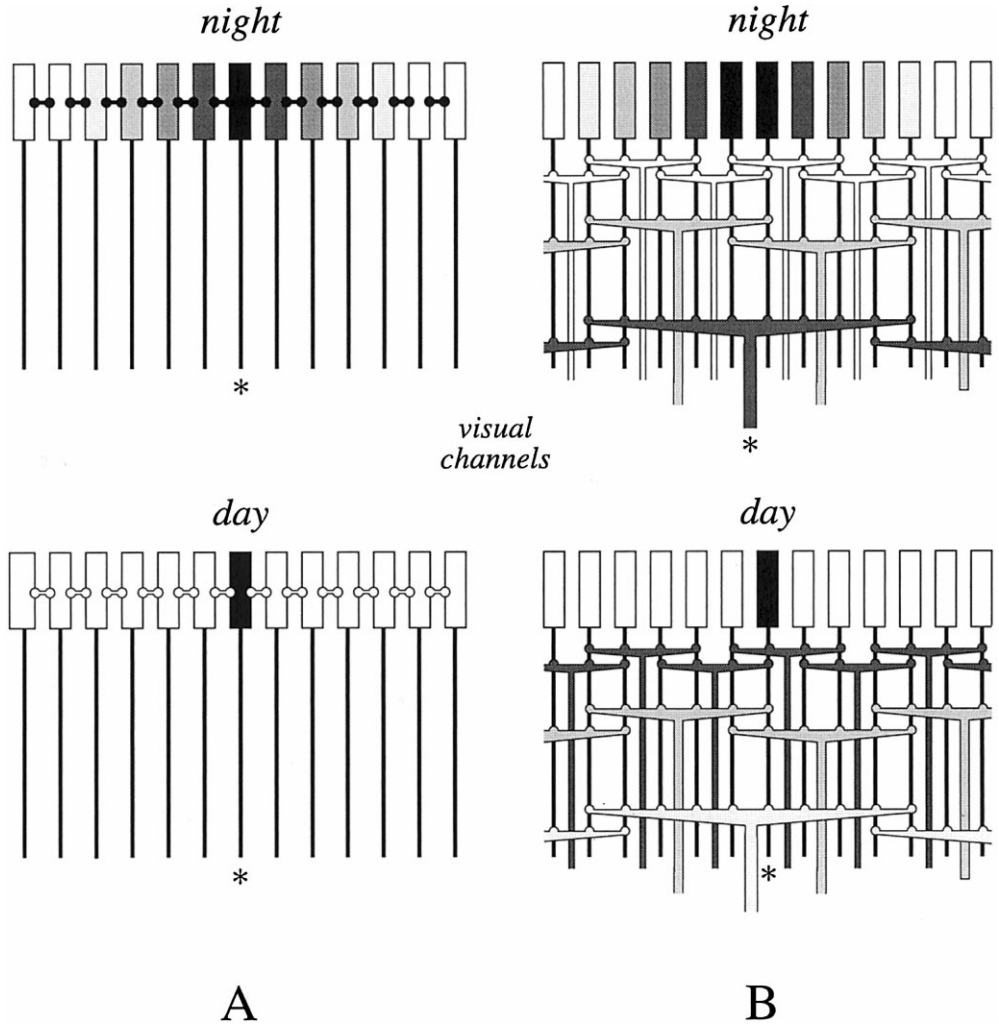

Fig. 9. Two neural schemes which could subserve spatial summation. (A) Inter-connection of visual channels by a class (or classes) of cells with widely spreading lateral fibres (dumb-bell shaped objects). At night (upper) this lateral interaction may be activated to connect visual channels (filled dumb-bells). The strength of the inter-connection may decrease from the central channel (*), as indicated by the paler shading of the channels. For clarity only a single summing channel is shown. During the day (lower) the lateral coupling may be inactivated (open dumb-bells), allowing all channels to operate in isolation with the highest possible spatial resolution. (B) Spatial summation of visual channel outputs by single cells, each of which has a wide dendritic field. Several spatial classes of wide-field cells may exist in parallel, possibly with many classes per visual channel (not indicated in the figure for clarity). At night (upper), the cells with the widest summation field (darkly shaded) receive the most light and have the highest signal-to-noise ratios: their high sensitivities and low spatial resolution dominate vision. The summation may be greatest at the centre of their receptive fields, and weaken with distance from the channel centre, as indicated by the paler shading of the channels (as seems to be the case with rod summation by ganglion cells in frog and toad retinas: Donner & Grönholm, 1984; Copenhagen et al., 1990). For clarity only a single summing channel is shown (*). Cells with smaller dendritic fields may still contribute to vision, but to a lesser extent because of their lower photon catch. If the dendritic field is too small, the photon catch will be too low to be reliable and the cell will not contribute (unshaded cells). During the day (lower), all channels can act in isolation to provide the maximum spatial resolution. The wide-field cells are still active, but those with narrower summation fields dominate vision (as indicated by their darker shading).

to those with widest dendritic field (most summation and worst resolution). At high light intensities all classes of cells receive sufficient photons to give reliable responses and the highest possible spatial resolution is achieved. As light intensities fall, the cell classes with the smallest dendritic fields receive insufficient photons from summation to give a reliable response, so their contribution to vision (the perception of finer spatial details) drops out. As the light intensity continues to fall, only those classes with dendritic fields large enough to catch a reliable number of photons remain operational, and vision becomes progressively coarser. This scheme, first proposed by Pirenne and Denton in 1952, was used to explain the dependence of acuity on light intensity in the periphery of the human eye. It is currently the best model to explain the cortical summation of ganglion cell channels in the foveal visual fields of cats and monkeys (see Appendix A).

Acknowledgements

I am extremely grateful to my friend and colleague Dan-Eric Nilsson for much inspiration, many long and fruitful discussions and for critically reading the manuscript. I am also deeply indebted to Hans van Hateren, who also critically read the manuscript, and whose masterful insights alerted me to several areas of potential ambiguity. The suggestions of two anonymous referees greatly improved the manuscript. I would also like to thank Rüdiger Wehner and Thomas Labhart for several helpful suggestions. Joaquin Arroyo Luna drew the toads. I am very grateful for the ongoing support of the Swedish Natural Science Research Council. This paper was completed during a Fellowship at the Institute of Advanced Study in Berlin, whose support and marvellous working environment I am particularly grateful for.

Appendix A. Visual channels in vertebrate eyes

In order to make a meaningful comparison of spatial summation between compound eyes and vertebrate camera eyes I defined visual channels in the latter to be specified by the matrix of retinal ganglion cells. Here I justify this definition.

As already mentioned in Section 2, it is the matrix of ganglion cells (and not photoreceptors) which sets the sampling matrix in vertebrate eyes, and determines the shape, size and location of the fovea(s) (Hughes, 1977). Despite this fact, it is necessary to account for another very important summation which takes place prior to the ganglion cells. Throughout the retina, the ganglion cells receive inputs (via bipolar cells) from pools of rods or cones, in some cases from as many as a thousand. The size of this pool increases with retinal eccentricity, and in some species also with decreasing ambient light intensity (e.g. Barlow, 1958; Enroth-Cugell & Robson, 1966; Donner, 1981; Derrington & Lennie, 1982; Troy, Oh & Enroth-Cugell, 1993). Because a ganglion cell receives input from a large pool, this is equivalent to the ganglion cell spatially summing signals from all of these photoreceptors, thus dramatically improving signal strength. The size of the photoreceptor pool effectively sets the size (and sensitivity) of the receptive field of a single ganglion cell at a given point in the retina (Copenhagen et al., 1990). In higher vertebrates, the only exception to this is in the central region of the fovea, where ganglion cells receive inputs from single cones (and then only the P-ganglion cells: the M-ganglion cells receive inputs from small pools of cones). Even though the ganglion cells determine the retina's sampling matrix, the importance of this initial summation of photoreceptor signals cannot be underestimated, especially in dim light. This spatial summation has been carefully accounted for in the model by assuming that each photoreceptor pool has a Gaussian-shaped sensitivity profile (Donner & Grönholm, 1984; Copenhagen et al., 1990) and a particular photoreceptor density (see Appendix B). Because the signal carried by the ganglion cell is already optimised by a preceding summation, it may render any further spatial summation between ganglion cell channels unnecessary (as we have concluded for sedentary toads, although the conclusion may be different for animals experiencing higher image velocities). Nevertheless, there is good evidence that such a second summation does occur. This comes from comparing the receptive fields of ganglion cells in the fovea with the receptive fields of cortical cells that have a foveal receptive field. Small photoreceptor pools give foveal ganglion cells small receptive fields. However, in cats and monkeys, the cortical cells receiving projections from the fovea are found to have a variety of receptive field sizes, with many cells having vastly larger receptive fields than expected from the underlying matrix of foveal ganglion cells (Tootell, Silverman & De Valois, 1981; De Valois, Albrecht & Thorell, 1982; Tootell, Silverman, Switkes & De Valois, 1982). Furthermore, in cats, foveal cortical cells with smaller receptive fields respond only at higher light intensities, whilst those with larger fields continue to respond even at lower intensities (Hess, 1990). These findings suggest the presence of Pirenne and Denton (1952) spatial summation between the channels defined by ganglion cells in cats and monkeys (see Fig. 9B).

Appendix B. Derivation of N and σ_D^2 in compound and camera eyes

In the derivations which follow, all symbols and their units are defined in Table 1, unless otherwise stated.

Derivation of N with spatial summation

The number N of photons captured by an output visual channel (Fig. 3) during one integration time Δt is the product of the light intensity (I), the number of lenses contributing light equally to each input channel (n_f), the area of each lens aperture ($\pi/4 \cdot A^2$, where A is the aperture diameter), the integration time Δt, the efficiency of the eye in detecting photons entering the aperture (γ) and the total solid-angular subtense of all the photoreceptors contributing to the output channel (Ω_T):

$$N = \frac{\pi}{4} A^2 n_f \, \Delta t \, \Omega_T \, \gamma \, I \tag{A1}$$

The number of lenses n_f is really only relevant to compound eyes. In superposition eyes n_f could reach 1000, whereas in apposition eyes it equals one (by definition). It obviously equals one in camera eyes too, and for their equations it is therefore omitted as a

parameter. The fraction of absorbed white light is given by (Warrant & Nilsson, 1998)

$$\gamma = \kappa\tau\left(\frac{kl}{2.3+kl}\right) \tag{A2}$$

where k is the absorption coefficient of the photoreceptor, κ is the quantum capture efficiency of the transduction process, τ is the fraction of incident light transmitted by the optics of the eye and l is the photoreceptor length. The bracketed term in Eq. (A2) is the absorptance of white light in the channel (Warrant & Nilsson, 1998). In previous studies, the absorptance has always been given by $(1-e^{-kl})$, but this is only valid for monochromatic stimulation. Only animals living in deep water experience near-monochromatic (blue) light.

The total solid-angular subtense of the output channel is given by

$$\Omega_T = n_r\, n_p\, \Omega, \tag{A3}$$

where n_r is the number of photoreceptors associated with each input channel (one in compound eyes, hundreds or even thousands in the rod pools feeding into ganglion cells), n_p is the number of input channels summing effectively equally and Ω is the solid angular subtense of each photoreceptor. For a photoreceptor of diameter d in an eye of focal length f, Ω is given by (Snyder, 1977, 1979)

$$\Omega = 1.13\left(\frac{d}{f}\right)^2, \tag{A4}$$

which is equivalent to the volume under a Gaussian function of half-width d/f radians. To calculate n_p we first calculate the number of input channels (n) encompassed by the three-dimensional Gaussian spatial summation function (Fig. 4). Like all Gaussians, the flanks of the summation function never reach zero. I will define the farthest extent of summation to occur when the summation function falls to 1% of its on-axis amplitude. The summation formulation I present in this paper assumes a perfect linear summation of signals from each participating channel. This means that the signal is proportional to n_p and the photon shot noise is proportional to $\sqrt{n_p}$.

If a summation function $f_p(\phi)$ of half-width $\Delta\rho_p$ varies with angle (ϕ) according to (Götz, 1964)

$$f_p(\phi) = \exp\left[-2.77\left(\frac{\phi}{\Delta\rho_p}\right)^2\right], \tag{A5}$$

then it can be easily shown that when $f_p(\phi) = 0.01$, the circular angular area A_b encompassed by the base of the three-dimensional summation function is given by

$$A_b = 4.050\ \Delta\rho_p^2. \tag{A6}$$

The number of input channels (n) that fill this area is then simply A_b divided by the circular angular area occupied by a single channel ($\pi/4\cdot\Delta\phi^2$):

$$n = 5.157\left(\frac{\Delta\rho_P}{\Delta\phi}\right)^2. \tag{A7}$$

Because each of these n channels obviously do not contribute equally to the summation, we have to calculate the effective number (n_p) that do contribute equally. Had all the channels contributed equally, the summation function would have actually been a cylinder (in three dimensions), with a volume $A_b\ h$, where h, the height of the cylinder, is simply one (the on-axis amplitude of the summation function: Eq. (A5)). The actual summation function, out to 1% amplitude, has a volume equal to $1.12\ \Delta\rho_p^2$. We can make a good estimate of n_p by multiplying n by the ratio of the volumes of the actual summation function and the cylindrical summation function. Using Eqs. (A6) and (A7) we then obtain

$$n_p = 1.426\left(\frac{\Delta\rho_p}{\Delta\phi}\right)^2. \tag{A8}$$

For vertebrate eyes we must also calculate n_r, the effective number of photoreceptors contributing equally to each input channel. The receptive field of a toad ganglion cell can be modelled as a Gaussian. According to this model, n_r is simply (Copenhagen et al., 1990):

$$n_r = 1.13\ \delta\ \Delta\rho^2, \tag{A9}$$

where δ is the photoreceptor density in the retina (deg^{-2}) and $\Delta\rho$ is the half-width of the ganglion cell receptive field.

We can now use Eqs. (A1), (A2), (A3), (A4) and (A8) to derive N for compound eyes (noting that $n_r = 1$),

$$N = 1.269\ n_f\,\kappa\tau\left(\frac{kl}{2.3+kl}\right)\Delta t\left(\frac{\Delta\rho_p\, dA}{\Delta\phi f}\right)^2 I$$

and further including Eq. (A9), we can do the same for vertebrate camera eyes (noting that $n_f = 1$),

$$N = 1.430\ \delta\ \kappa\tau\left(\frac{kl}{2.3+kl}\right)\Delta t\ \Delta\rho^2\left(\frac{\Delta\rho_P\, dA}{\Delta\phi\, f}\right)^2 I$$

Derivation of σ_D^2 with spatial summation

The total dark variance σ_D^2 is simply the product of the specific dark variance (ω), the total volume (V) of photoreceptive membrane contributing to the output channel (Fig. 3), and the integration time Δt:

$$\sigma_D^2 = \omega\ V\ \Delta t, \tag{A10}$$

where V is given by the total number of contributing photoreceptors multiplied by the volume of a single photoreceptor ($\pi/4\ d^2 l$):

$$V = \frac{\pi}{4}\, n_r\, n_p\, d^2\, l \tag{A11}$$

All symbols have their usual meanings. We can now use Eqs. (A8), (A10) and (A11) to derive σ_D^2 for compound eyes (noting that $n_r = 1$),

$$\sigma_D^2 = 1.131\ \omega\ l\ \Delta t\left(\frac{\Delta\rho_p\, d}{\Delta\phi}\right)^2,$$

and further including Eq. (A9), we can do the same for vertebrate camera eyes,

$$\sigma_D^2 = 1.269\ \omega\ \delta\ l\ \Delta t\ \Delta\rho^2\left(\frac{\Delta\rho_P\, d}{\Delta\phi}\right)^2.$$

Derivation of N and σ_D^2 without spatial summation

The equations for N and σ_D^2 in the absence of summation (Eqs. (6a), (7a), (8a) and (9a)) are derived in exactly the same way as above except that the effective number of channels contributing equally to spatial summation is set to one (i.e. $n_p = 1$).

References

Aho, A.-C., Donner, K., Hydén, C., Larsen, L. O., & Reuter, T. (1988). Low retinal noise in animals with low body temperature allows high visual sensitivity. *Nature* (*London*), *334*, 348–350.

Aho, A.-C., Donner, K., Helenius, S., Larsen, L. O., & Reuter, T. (1993). Visual performance of the toad (*Bufo bufo*) at low light levels: retinal ganglion cell responses and prey-catching accuracy. *Journal of Comparative Physiology A*, *172*, 671–682.

Atick, J. J., & Redlich, A. N. (1992). What does the retina know about natural scenes? *Neural Computation*, *4*, 196–210.

Barlow, H. B. (1956). Retinal noise and absolute threshold. *Journal of the Optical Society of America*, *46*, 634–639.

Barlow, H. B. (1958). Temporal and spatial summation in human vision at different background intensities. *Journal of Physiology*, *141*, 337–350.

Barlow, H. B. (1965). Optic nerve impulses and Webers Law. *Cold Spring Harbour Symposia on Quantitative Biology*, *30*, 539–546.

Bryceson, K. P., & McIntyre, P. D. (1983). Image quality and acceptance angle in a reflecting superposition eye. *Journal of Comparative Physiology*, *151*, 367–380.

Burr, D. C. (1980). Motion smear. *Nature*, *284*, 164–165.

Burr, D.C. (1991). Human sensitivity to flicker and motion. In: J.J. Kulikowski, V. Walsh, & I.J. Murray, *Vision and visual dysfunction*, *vol. 5*, *Limits of vision* (pp 147–159). Houndmills, & London: Macmillan Press, Scientific and Medical.

Burr, D. C., & Ross, J. (1982). Contrast sensitivity at high velocities. *Vision Research*, *23*, 3567–3569.

Chapman, R. F. (1980). *The insects. Structure and function*. London: Hodder and Stoughton.

Copenhagen, D. R., Hemilä, S., & Reuter, T. (1990). Signal transmission through the dark-adapted retina of the toad. *Journal of General Physiology*, *95*, 717–732.

Derrington, A. M., & Lennie, P. (1982). The influence of temporal frequency and adaptation level on receptive field organization of retinal ganglion cells in cat. *Journal of Physiology*, *333*, 343–366.

De Valois, R. L., Albrecht, D. G., & Thorell, L. G. (1982). Spatial frequency selectivity of cells in macaque visual cortex. *Vision Research*, *22*, 545–559.

De Valois, R. L., & De Valois, K. K. (1990). *Spatial vision*. Oxford: Oxford University Press.

Donner, K. (1981). Receptive fields of frog retinal ganglion cells: response formation and light-dark-adaptation. *Journal of Physiology*, *319*, 131–142.

Donner, K. (1987). Adaptation-related changes in the spatial and temporal summation of frog retinal ganglion cells. *Acta Physiologica Scandinavica*, *131*, 479–487.

Donner, K. (1989). Visual latency and brightness: an interpretation based on the responses of rods and ganglion cells in the frog retina. *Visual Neuroscience*, *3*, 39–51.

Donner, K. (1992). Noise and the absolute thresholds of cone and rod vision. *Vision Research*, *32*, 853–866.

Donner, K., & Grönholm, M. L. (1984). Centre and surround excitation in the receptive fields of frog retinal ganglion cells. *Vision Research*, *24*, 1807–1819.

Donner, K., Koskelainen, A., Djupsund, K., & Hemilä, S. (1995). Changes in retinal time scale under background light: observations on rods and ganglion cells in the frog retina. *Vision Research*, *35*, 2255–2266.

Dvorak, D., & Snyder, A. W. (1978). The relationship between visual acuity and illumination in the fly, *Lucilia sericata*. *Zeitschrift für Naturforschung*, *33C*, 139–143.

Dubs, A. (1982). The spatial integration of signals in the retina and lamina of the fly compound eye under different conditions of luminance. *Journal of Comparative Physiology A*, *146*, 321–343.

Dubs, A., Laughlin, S. B., & Srinivasan, M. V. (1981). Single photon signals in fly photoreceptors and first order interneurons at behavioural threshold. *Journal of Physiology*, *317*, 317–334.

Doujak, F. E. (1985). Can a shore crab see a star? *Journal of Experimental Biology*, *166*, 385–393.

Enroth-Cugell, C., & Robson, J. G. (1966). The contrast sensitivity of retinal ganglion cells of the cat. *Journal of Physiology*, *187*, 517–552.

Eckert, M. P., & Buchsbaum, G. (1993). Efficient coding of natural time-varying images in the early visual system. *Proceedings of the Royal Society of London B*, *339*, 385–395.

Field, D. J. (1987). Relations between the statistics of natural images and the response properties of cortical cells. *Journal of the Optical Society of America A*, *4*, 2379–2394.

Götz, K. G. (1964). Optomotorische untersuchung des visuellen systems einiger augenmutanten der fruchtfliege Drosophila. *Kybernetik*, *2*, 77–92.

Hallett, P. E. (1991). Some limitations to human peripheral vision. In: J. J. Kulikowski, V. Walsh,, & I. J. Murray, *Vision and visual dysfunction*, vol. 5: Limits of vision (pp. 44–80). Houndmills, & London: Macmillan Press, Scientific and Medical.

van Hateren, J. H. (1992). Real and optimal neural images in early vision. *Nature*, *360*, 68–69.

van Hateren, J. H. (1992). Theoretical predictions of spatiotemporal receptive fields of fly LMCs, and experimental validation. *Journal of Comparative Physiology A*, *171*, 157–170.

van Hateren, J. H. (1992). A theory of maximising sensory information. *Biological Cybernetics*, *68*, 23–29.

van Hateren, J. H. (1993). Spatiotemporal contrast sensitivity of early vision. *Vision Research*, *33*, 257–267.

van Hateren, J. H. (1993). Three modes of spatiotemporal preprocessing by eyes. *Journal of Comparative Physiology A*, *172*, 583–591.

van Hateren, J. H. (1993). Spatial, temporal and spectral pre-processing for colour vision. *Proceedings of the Royal Society of London B*, *251*, 61–68.

Hess, R. F. (1990). Rod-mediated vision: role of post-receptoral filters. In R. F. Hess, L. T. Sharpe, & K. Nordby, *Night vision*. Cambridge: Cambridge University Press, 3–48.

Horridge, G. A., & Sandeman, D. C. (1964). Nervous control of optokinetic responses in the crab *Carcinus*. *Proceedings of the Royal Society of London B*, *161*, 216–246.

Horridge, G. A., & Marcelja, L. (1992). On the existence of 'fast' and 'slow' directionally sensitive motion detector neurons in insects. *Proceedings of the Royal Society of London B*, *248*, 47–54.

Howard, J., & Snyder, A. W. (1983). Transduction as a limitation on compound eye function and design. *Proceedings of the Royal Society of London B*, *217*, 287–307.

Hughes, A. (1977). The topography of vision in mammals of contrasting life style: comparative optics and retinal organisation. In:

F. Crescitelli, *Handbook of sensory physiology*, vol. VII/5 (pp. 613–756). Berlin: Springer.

Kulikowski, J. J., & Tolhurst, D. J. (1973). Psychophysical evidence for sustained and transient detectors in human vision. *Journal of Physiology* (*London*), *232*, 149–162.

Land, M.F. (1981). Optics and vision in invertebrates. In: H. Autrum, *Handbook of sensory physiology*, vol. VII/6B (pp. 471–592). Berlin: Springer.

Land, M. F. (1989). Variations in the structure and design of compound eyes. In D. G. Stavenga, & R. C. Hardie, *Facets of vision*. Berlin: Springer, 90–111.

Larsen, L. O., & Pedersen, J. N. (1982). The snapping response of the toad, *Bufo bufo*, towards prey dummies at very low light intensities. *Amphibia-Reptilia*, *2*, 321–327.

Laughlin, S.B. (1981) Neural principles in the peripheral visual systems of invertebrates. In: H. Autrum, *Handbook of sensory physiology*, vol. VII/6B (pp. 133–280). Berlin: Springer.

Laughlin, S. B. (1990). Invertebrate vision at low luminances. In R. F. Hess, L. T. Sharpe, & K. Nordby, *Night vision*. Cambridge: Cambridge University Press, 223–250.

Laughlin, S. B. (1992). Retinal information capacity and the function of the pupil. *Ophthalmic and Physiological Optics*, *12*, 161–164.

Laughlin, S. B., & Lillywhite, P. G. (1982). Intrinsic noise in locust photoreceptors. *Journal of Physiology*, *332*, 25–45.

Lillywhite, P. G. (1977). Single photon signals and transduction in an insect eye. *Journal of Comparative Physiology*, *122*, 189–200.

Lythgoe, J. N. (1979). *The ecology of vision*. Oxford: Clarendon Press.

Moeller, J. F., & Case, J. F. (1994). Properties of visual interneurons in a deep-sea mysid, *Gnathophausia ingens*. *Marine Biology*, *119*, 211–219.

Moeller, J. F., & Case, J. F. (1995). Temporal adaptations in visual systems of deep-sea crustaceans. *Marine Biology*, *123*, 47–54.

Murray, I., Macana, F., & Kulikowski, J. J. (1983). Contribution of two movement detecting mechanisms to central and peripheral vision. *Vision Research*, *23*, 151–159.

Nalbach, H.-O. (1989). Three temporal frequency channels constitute the dynamics of the optokinetic system of the crab, *Carcinus maenus* (L.). *Biological Cybernetics*, *61*, 59–70.

Nilsson, D.-E. (1989). Optics and evolution of the compound eye. In D. G. Stavenga, & R. C. Hardie, *Facets of vision*. Berlin: Springer, 30–73.

Nilsson, D.-E., & Odselius, R. (1981). A new mechanism for light-dark adaptation in the *Artemia* compound eye (Anostraca, Crustacea). *Journal of Comparative Physiology*, *143*, 389–399.

Nilsson, D.-E., & Ro, A.-I. (1994). Did neural pooling for night vision lead to the evolution of neural superposition eyes? *Journal of Comparative Physiology A*, *175*, 289–302.

Pick, B., & Buchner, E. (1979). Visual movement detection under light- and dark-adaptation in the fly, *Musca domestica*. *Journal of Comparative Physiology*, *134*, 45–54.

Pirenne, M. H. (1967). *Vision and the eye*. London: Chapman and Hall.

Pirenne, M. H., & Denton, E. J. (1952). Accuracy and sensitivity of the human eye. *Nature*, *170*, 1039–1042.

Pyza, E., & Meinertzhagen, I. A. (1993). Daily and circadian rhythms of synaptic frequency in the first visual neuropile of the houseflys (*Musca domestica* L.) optic lobe. *Proceedings of the Royal Society of London B*, *254*, 97–105.

Raynauld, J. P., Laviolette, J. R., & Wagner, H.-J. (1979). Goldfish retina: a correlate between cone activity and morphology of the horizontal cell in cone pedicules. *Science*, *204*, 1436–1438.

Roebroek, J. G. H., & Stavenga, D. G. (1990). On the effective optical density of the pupil mechanism in fly photoreceptors. *Vision Research*, *30*, 1235–1242.

Sandeman, D. C., & Erber, J. (1976). The detection of real and apparent motion by the crab *Leptograpsus variegatus*. *Journal of Comparative Physiology*, *112*, 181–188.

Schuling, F. H., Mastebroek, H. A. K., Bult, R., & Lenting, B. P. M. (1989). Properties of elementary movement detectors in the fly *Calliphora erythrocephala*. *Journal of Comparative Physiology A*, *165*, 179–192.

Shapley, R., & Enroth-Cugell, C. (1984). Visual adaptation and retinal gain controls. In N. O. Osborne, & G. J. Chader, *Progress in retinal research*, Vol. 3. London: Pergamon Press, 263–346.

Sharpe, L. T. (1990). The light-adaptation of the human rod visual system. In R. F. Hess, L. T. Sharpe, & K. Nordby, *Night vision*. Cambridge: Cambridge University Press, 49–124.

Shaw, S. R. (1984). Early visual processing in insects. *Journal of Experimental Biology*, *112*, 225–251.

Snyder, A. W. (1977). Acuity of compound eyes: physical limitations and design. *Journal of Comparative Physiology*, *116*, 161–182.

Snyder, A. W. (1979). Physics of vision in compound eyes. In: H. Autrum, *Handbook of sensory physiology*, vol. VII/6A (pp. 225–313). Berlin: Springer.

Snyder, A. W., Stavenga, D. G., & Laughlin, S. B. (1977). Spatial information capacity of compound eyes. *Journal of Comparative Physiology*, *116*, 183–207.

Snyder, A. W., Laughlin, S. B., & Stavenga, D. G. (1977). Information capacity of eyes. *Vision Research*, *17*, 1163–1175.

Srinivasan, M. V., & Bernard, G. D. (1975). The effect of motion on visual acuity of the compound eye: a theoretical analysis. *Vision Research*, *15*, 515–525.

Srinivasan, M. V., & Dvorak, D. R. (1980). Spatial processing of visual information in the movement-detecting pathway of the fly. *Journal of Comparative Physiology*, *140*, 1–23.

Srinivasan, M. V., Laughlin, S. B., & Dubs, A. (1982). Predictive coding: a fresh view of coding in the retina. *Proceedings of the Royal Society of London B*, *216*, 427–459.

Strausfeld, N. J. (1989). Beneath the compound eye: neuroanatomical analysis and physiological correlates in the study of insect vision. In D. G. Stavenga, & R. C. Hardie, *Facets of vision*. Berlin: Springer, 317–359.

Strausfeld, N. J., & Campos-Ortega, J. A. (1977). Vision in insects: pathways possibly underlying neural adaptation and lateral inhibition. *Science*, *195*, 894–897.

Tolhurst, D. J. (1973). Separate channels for the analysis of the shape and the movement of a moving visual stimulus. *Journal of Physiology* (*London*), *231*, 385–402.

Tootell, R. B. H., Silverman, M. S., & De Valois, R. L. (1981). Spatial frequency columns in primary visual cortex. *Science*, *214*, 813–815.

Tootell, R. B. H., Silverman, M. S., Switkes, E., & De Valois, R. L. (1982). Deoxyglucose analysis of retinotopic organization in primate striate cortex. *Science*, *218*, 902–904.

Troy, J. B., Oh, J. K., & Enroth-Cugell, C. (1993). Effect of ambient illumination on the spatial properties of the centre and surround of Y-cell receptive fields. *Visual Neuroscience*, *10*, 753–764.

Warrant, E. J., & McIntyre, P. D. (1990). Screening pigment, aperture and sensitivity in the dung beetle superposition eye. *Journal of Comparative Physiology A*, *167*, 805–815.

Warrant, E. J., & McIntyre, P. D. (1990). Limitations to resolution in superposition eyes. *Journal of Comparative Physiology A*, *167*, 785–803.

Warrant, E. J., & McIntyre, P. D. (1991). Strategies for retinal design in arthropod eyes of low F-number. *Journal of Comparative Physiology A*, *168*, 499–512.

Warrant, E. J., & McIntyre, P. D. (1992). The trade-off between resolution and sensitivity in compound eyes. In R. B. Pinter, & B. Nabet, *Nonlinear vision*. Boca Raton: CRC Press, 391–421.

Warrant, E. J., & McIntyre, P. D. (1993). Arthropod eye design and the physical limits to spatial resolving power. *Progress in Neurobiology*, *40*, 413–461.

Warrant, E. J., & McIntyre, P. D. (1996). The visual ecology of pupillary action in superposition eyes. *Journal of Comparative Physiology A*, *178*, 75–90.

Warrant, E. J., Porombka, T., & Kirchner, W. H. (1996). Neural image enhancement allows honeybees to see at night. *Proceedings of the Royal Society of London B*, *263*, 1521–1526.

Warrant, E. J., & Nilsson, D.-E. (1998). Absorption of white light in photoreceptors. *Vision Research*, *38*, 195–207.

Wehner, R. (1981). Spatial vision in arthropods. In: H. Autrum, *Handbook of sensory physiology*, vol. VII/6C (pp. 287–616). Berlin: Springer.

Weiler, R., Kohler, K., Kirsch, M., & Wagner, H.-J. (1988). Glutamate and dopamine modulate synaptic plasticity in horizontal cell dendrites of fish retina. *Neuroscience Letters*, *87*, 205–209.

Williams, D. S. (1982). Ommatidial structure in relation to turnover of photoreceptor membrane in the locust. *Cell and Tissue Research*, *225*, 595–617.

Williams, D. S. (1983). Changes of photoreceptor performance associated with the daily turnover of photoreceptor membrane in the locust. *Journal of Comparative Physiology*, *150*, 509–519.

Wilson, M. (1975). Angular sensitivity of light and dark adapted locust retinula cells. *Journal of Comparative Physiology*, *97*, 323–328.

Wilson, M., Garrard, P., & McGinness, S. (1978). The unit structure of the locust compound eye. *Cell and Tissue Research*, *195*, 205–226.

Yang, E.C. (1994). Processing of spectral information in the dragonfly lamina. PhD thesis, Australian National University, Canberra.